Materials Research Letters

ISSN: (Print) (Online) Journal homepage: https://www.tandfonline.com/loi/tmrl20

High entropy oxide (Co,Cu,Mg,Ni,Zn)O exhibits grain size dependent room temperature deformation

Xin Wang, Justin Cortez, Alexander D. Dupuy, Julie M. Schoenung & William J. Bowman

To cite this article: Xin Wang, Justin Cortez, Alexander D. Dupuy, Julie M. Schoenung & William J. Bowman (2023) High entropy oxide (Co,Cu,Mg,Ni,Zn)O exhibits grain size dependent room temperature deformation, Materials Research Letters, 11:3, 196-204, DOI: 10.1080/21663831.2022.2135409

To link to this article: https://doi.org/10.1080/21663831.2022.2135409

MATER. RES. LETT.
2023, VOL. 11, NO. 3, 196–204
https://doi.org/10.1080/21663831.2022.2135409

MATERIALS RESEARCH LETTERS
Taylor & Francis
Taylor & Francis Group

ORIGINAL REPORTS

High entropy oxide (Co,Cu,Mg,Ni,Zn)O exhibits grain size dependent room temperature deformation

Xin Wang[a], Justin Cortez[a], Alexander D. Dupuy [a], Julie M. Schoenung[a] and William J. Bowman[a,b]

[a]Department of Materials Science and Engineering, University of California, Irvine, CA, USA; [b]Irvine Materials Research Institute, University of California, Irvine, CA, USA

ABSTRACT

Despite their vast composition space and promising properties, little is known about the fundamental mechanical behavior of high entropy oxides (HEOs). Here we provide experimental evidence of the nanoscale origin of room temperature deformation in (Co,Cu,Mg,Ni,Zn)O HEOs with different grain sizes. We find that micron-grain (Co,Cu,Mg,Ni,Zn)O deforms predominately through extensive $\frac{1}{2}<110>\{1\text{–}10\}$ dislocation slip manifesting as discrete slip bands. Nano-grain (Co,Cu,Mg,Ni,Zn)O, in addition to moderate dislocation slip activity, deforms through grain boundary sliding and intergranular cracking. The significant dislocation-mediated deformation and grain size dependent behavior demonstrates that HEOs have the potential for diverse and highly tailorable mechanical behavior.

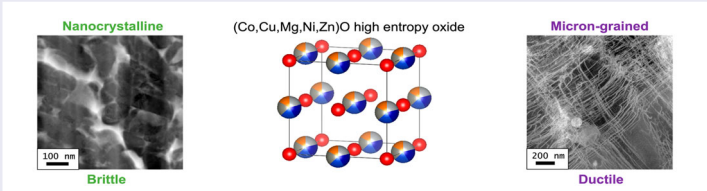

IMPACT STATEMENT

High entropy oxides (Co,Cu,Mg,Ni,Zn)O exhibit grain size dependent room temperature deformation, with micron-grain samples displaying significant potential for dislocation-mediated deformation and nanocrystalline samples exhibiting grain boundary sliding and micro-cracking.

ARTICLE HISTORY
Received 28 June 2022

KEYWORDS
High entropy oxide (HEO); nanoscratch; deformation; dislocation; grain size effect

Introduction

The emerging field of complex concentrated materials establishes an unconventional materials design strategy by exploring the central domain of multicomponent phase diagrams. This new class of materials offers entropy-enhanced stability and compositionally tunable properties, which are required for the next generation of functional and structural applications. In 2015, the high entropy design strategy was first applied to oxide materials to produce high entropy oxides (HEO) (Co,Cu,Mg,Ni,Zn)O [1]. While our previous work indicates that (Co,Cu,Mg,Ni,Zn)O has a tendency to form secondary phases during heat treatment [2,3], a single-phase rocksalt solid solution structure can be retained down to the nanoscale after appropriate processing [3]. Since its first discovery, the potential of HEOs as cathodes, solid electrolytes, catalysts, and thermal insulators [4–6] has been explored, and the HEO concept has been extended to other ceramic systems such as carbides [7], silicides [8] and borides [9].

Engineering applications often require the materials in service to sustain mechanical loads. Therefore, careful consideration of the mechanical behavior of HEOs is necessary for them to be broadly useful. However, an inspection of the literature shows limited attention to this area. Desissa et al., for instance, observed that the hardness of dense (Co,Cu,Mg,Ni,Zn)O could reach as high as 16 GPa [10]. Hong et al. examined the bending strength of (Co,Cu,Mg,Ni,Zn)O and reported a trade-off between grain size and mechanical behavior [11]. Through experiments and modeling, Pitike et al. established that (Co,Cu,Mg,Ni,Zn)O has isotropic elastic properties [12]. Further, their calculations predict that (Co,Cu,Mg,Ni,Zn)O has the potential for meaningful

CONTACT William J. Bowman will.bowman@uci.edu Department of Materials Science and Engineering, University of California, Irvine, CA, USA; Irvine Materials Research Institute, University of California, Irvine, CA, USA

Supplemental data for this article can be accessed here. https://doi.org/10.1080/21663831.2022.2135409

plastic deformation compared to the constituent oxides, yet experimental evidence does not yet exist. Moreover, detailed knowledge of room temperature mechanical behavior and deformation mechanisms, such as dislocation structure and slip behavior, is lacking yet critical to properly design these materials for engineering applications.

Although not commonly observed in conventional ceramics at room temperature, dislocations in ceramics are known to impact a wide range of functional and mechanical properties, including the optical bandgap [13], thermal conductivity [14], ion transport [15,16], plasticity [13] and fracture toughness [17]. But unlike metals, ceramics rarely exhibit meaningful macroscopic ductility by slip processes at ambient temperatures, with a few exceptions such as MgO and CoO [18–20]. MgO, which is an ionic ceramic with a rocksalt crystal structure, deforms through two families of slip systems: $\frac{1}{2}<110>\{1\text{–}10\}$ and, at elevated temperatures, $\frac{1}{2}<110>\{001\}$ [20]. At room temperature, dislocation-mediated deformation of MgO is largely controlled by screw dislocations due to their higher lattice friction and lower mobility than edge dislocations [21]. Furthermore, grain boundary sliding as well as cracking will absorb mechanical energy during deformation [22]. The relative contributions of the deformation mechanisms can vary depending on the material system and is heavily influenced by the microstructure.

Due to their inherent brittleness, investigation of deformation in ceramics is difficult with conventional approaches, such as uniaxial tension and compression. A viable mechanical testing method is nanoscratch testing, which is a penetration based nanomechanical characterization technique [23,24]. A typical nanoscratch test involves penetrating a sample surface using a nanoindenter, followed by moving the indenter across the sample surface while controlling the downward penetration force [25]. The test generates a controlled region of penetration (the scratch groove) with a localized deformation zone (Figure 1(a)), which is well-suited for microscopic investigation to elucidate deformation mechanisms [23,24,26] and grain-size effects [24] in ceramics.

The goal of the present study is to explore the room temperature mechanical deformation behavior in (Co,Cu,Mg,Ni,Zn)O. We hypothesize that this emerging oxide may show room temperature plasticity, similar to MgO [20], and grain size dependent mechanical behavior [24]. Nanoscratch tests were performed on (Co,Cu,Mg,Ni,Zn)O with micron-scale and nanoscale grain sizes ('micron-grain' and 'nano-grain,' respectively). Post-deformation microstructures and defect atomic structures were characterized using (scanning) transmission electron microscopy (S/TEM) to reveal the deformation mechanisms. We show that the deformation behavior is predominantly dislocation slip for micron-grain HEO and grain boundary sliding and micro-cracking for nano-grain HEO. The differences in mechanical behavior between (Co,Cu,Mg,Ni,Zn)O and conventional rocksalt oxides are also discussed.

Results

Spark plasma sintering (SPS) consolidation of HEO nanopowders yielded highly dense, single-phase, bulk samples. Please see the Supplementary Information for detailed sample preparation methods and additional S/TEM and energy dispersive X-ray spectroscopy (EDS) characterization results. The nano-grain and micron-grain HEO samples have grain sizes of 75 nm and 1.4 μm, and relative density values of 95% and 99%, respectively. Pile-up of material ejected from the scratch groove is more obvious on both sides and at the end of the groove for micron-grain HEO than that for nano-grain HEO (Figure 1(b,c), respectively). From depth profiles at applied normal load values of 50 and 150 mN, it is evident that the nano-grain HEO shows deeper penetration depth than the micron-grain HEO (Figure 1(d,e)).

For micron-grain HEO at a normal load of ~150 mN, the deformation zone below the scratch, as shown in Figure 2(a), has a radius of ~8 μm; beyond this zone, undeformed equiaxed grains are observed (Figure 2(b)). Irregular grains (Figure 2(c)) and a high density of dislocations (Figure 2(d)) are observed in the deformation zone. Some variation in dislocation density is observed among the various grains in Figure 2(c), which is attributed to the differences in their crystal orientations. The dislocation density in the grain interior is calculated to be $\sim 3.4\times10^{14}$ m^{-2} following a line intercept method [27,28]. The region adjacent to the grain boundaries exhibits higher dislocation densities, which is not surprising since grain boundaries can serve as sources and barriers for dislocations [29]. As expected, the dislocation density in the 50 mN sample is lower (Fig. S1).

To characterize the slip modes in the micron-grain HEO, diffraction contrast imaging at selected two-beam and weak-beam conditions was performed (Figure 3). TEM images taken at the same area under two-beam bright-field and weak-beam dark-field conditions near a [011] zone axis with diffraction vectors g = 1–11 and g = −1–11 (Figure 3(a–d), respectively). Insets show the corresponding diffraction patterns, and diffraction vector directions are marked in the TEM images with arrows.

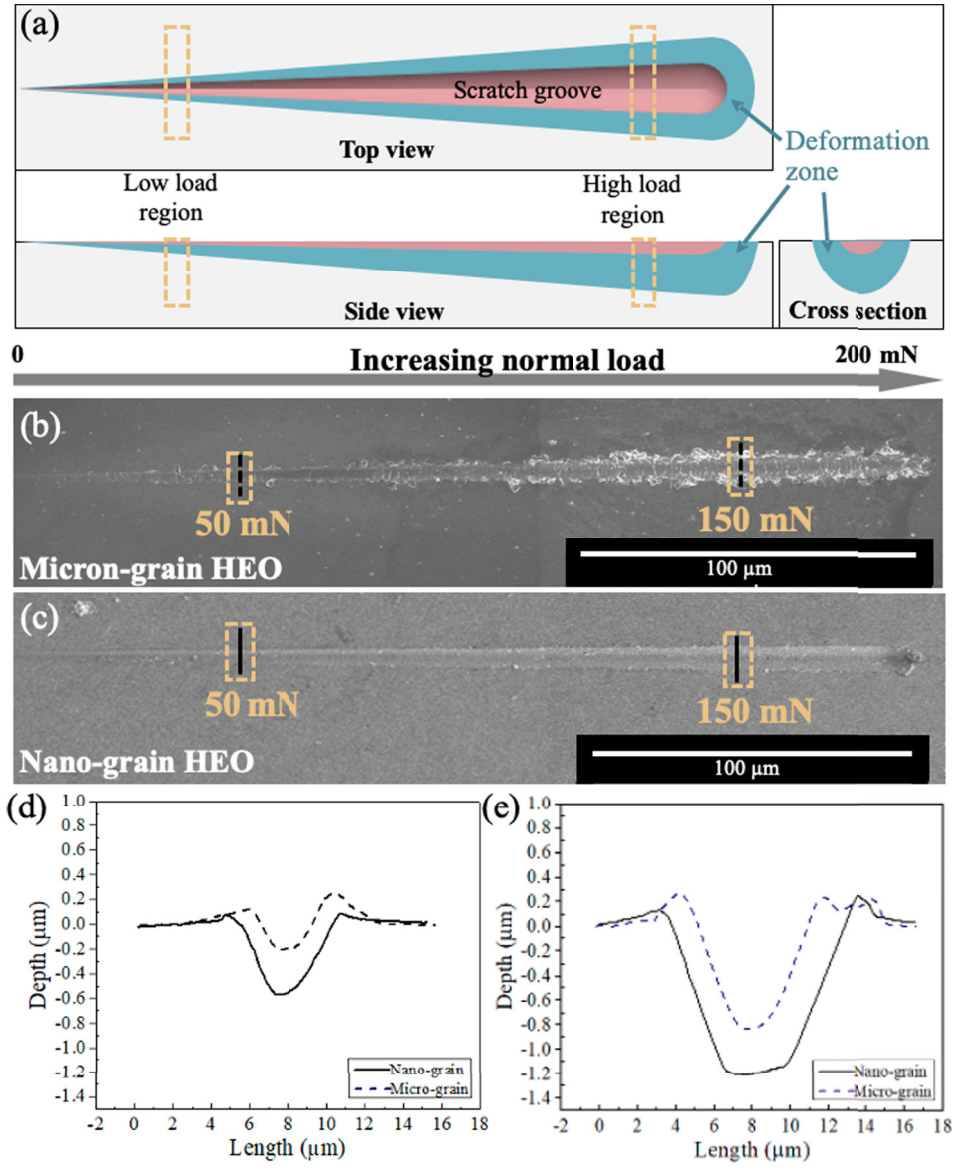

Figure 1. (a) Top, side and cross-sectional views of the nanoscratch track. (b, c) Post-nanoscratch SEM surface morphologies of micron-grain HEO and nano-grain HEO, respectively. (d, e) Depth profiles plotted for applied normal load values of 50 and 150 mN, respectively.

Most of the observed dislocations are confined to discrete slip bands (dashed white lines in Figure 3(a,c)). Based on the $\mathbf{g}\cdot\mathbf{b} = 0$ dislocation contrast vanishing criterion, the Burgers vectors for the dislocations are of the $\frac{1}{2} < 110 >$ type. The slip planes were found to be parallel to two of the orthogonal {1–10} planes by analyzing the inclined slip planes. We can thus conclude that the dislocation activity observed in our room temperature nanoscratch experiment is mainly governed by the $\frac{1}{2} < 110 >$ dislocation slip on {1–10} planes.

Most dislocations observed in the room temperature deformed micron-grained HEO are confined to slip bands (dashed lines in Figure 3(a,c)) indicating pronounced planar glide. Planar slip has been observed in metallic alloys [30–32] and to a limited extent in ceramics, including MgO [20,33] and $KNbO_3$ [34]. Several mechanisms have been proposed to explain the emergence of slip band behavior. One reason is the difficulty for dislocations to cross slip due to low stacking fault energy and high friction stress [35,36]. Moreover, slip band formation can be caused extrinsically by the presence of short range order (SRO) [32] or chemical clustering [37]. An initial dislocation will destroy the local SRO structure, resulting in glide plane softening. Subsequent dislocations will experience lower frictional forces in the vicinity of the initial dislocation, causing slip to become localized in a slip band. STEM EDS chemical analysis was performed on the micron-grained HEO at

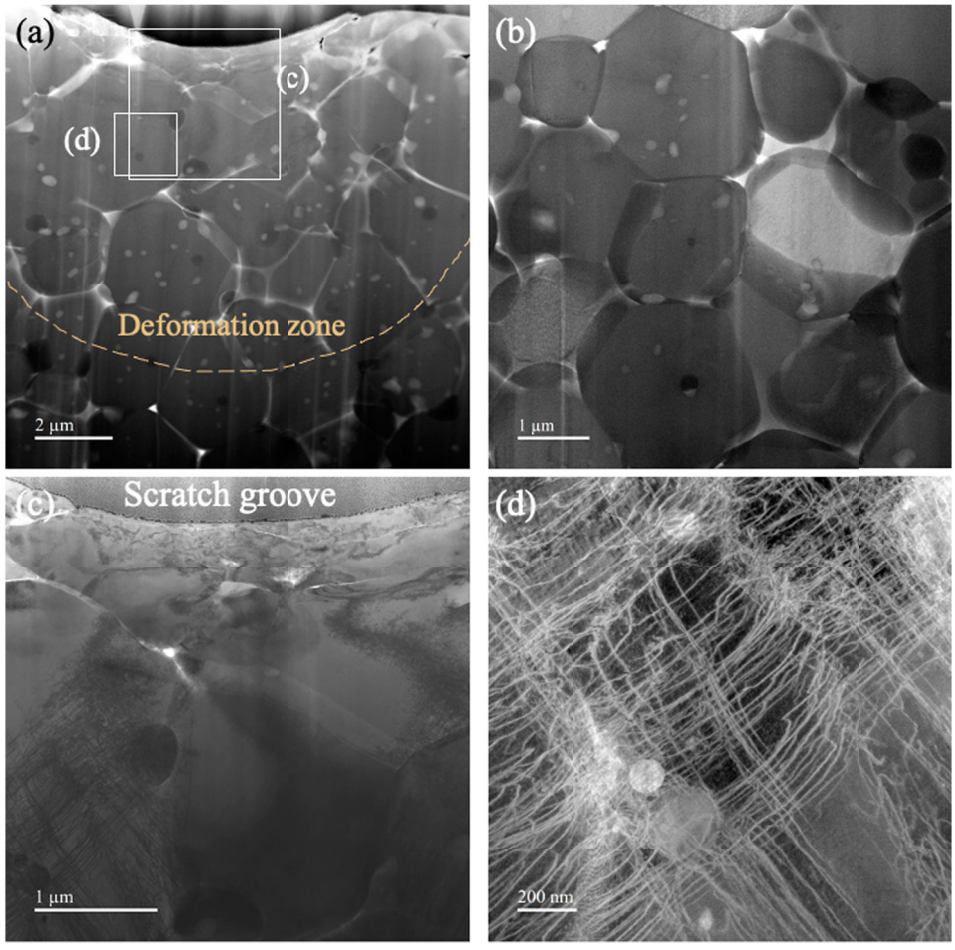

Figure 2. Cross section of the room temperature nanoscratch-tested micron-grain HEO at ~150 mN applied normal load: (a) Bright-field STEM image displaying the deformation zone below the scratch groove. (b) Bright-field STEM image showing the representative microstructure farther away from the scratch groove and outside the deformation zone. (c) Higher magnification bright-field STEM image of the region in (a). (d) Dark-field STEM image from the region marked in (a) showing a high density of dislocations formed during nanoscratch testing.

the intersection of slip bands, which show uniform distributions of all elements (Fig. S2). The presence of SRO is difficult to detect and has not been directly observed in micron-grain HEO. However, our previous work using atom probe tomography indicates that some amount of chemical clustering is present at the nanoscale [3]. We therefore ascribe the observed planar dislocation slip in micron-grain HEO to SRO or clustering, in addition to the high friction stress typical for ceramics.

To further analyze the dislocation core structures in micron-grain HEO, atomic resolution STEM imaging was performed (Figure 4). When imaged at a [001] zone axis, most of the dislocations appear as long straight lines along the {1–10} planes, which suggests they are screw dislocations. Only a small number of edge dislocations were observed close to a grain boundary (Figure 4(a,b)). Burgers circuit analyses show the Burgers vector of the edge dislocations is $\frac{1}{2} < 110 >$ (Figure 4(b)). Our observation that edge dislocations only appear near the grain boundaries is consistent with other materials that exhibit slip band behavior, such as MgO and Ti alloys [31,33]. Screw dislocations in micron-grain HEO had dislocation lines parallel to the {1–10} plane trace (Figure 4(c,d)). Inverse fast Fourier transformation (IFFT) image analysis of a region containing a screw dislocation revealed that the Burgers vector of the dislocation is also $\frac{1}{2} < 110 >$, parallel to the dislocation line (near vertical direction in Figure 4(d)). The significantly greater number of screw to edge dislocations in micron-grain HEO is consistent with the observation in single-crystalline MgO at room temperature [20,21], which has been attributed to the greater velocities of edge dislocations than screw dislocations under the same stress level [33,38,39].

The deformation behavior of the nano-grain HEO after room temperature nanoscratch testing was also investigated by S/TEM. At an applied normal load of ~50 mN (Fig. S3), the deformation zone beneath the scratch groove exhibits a lower concentration of cavities

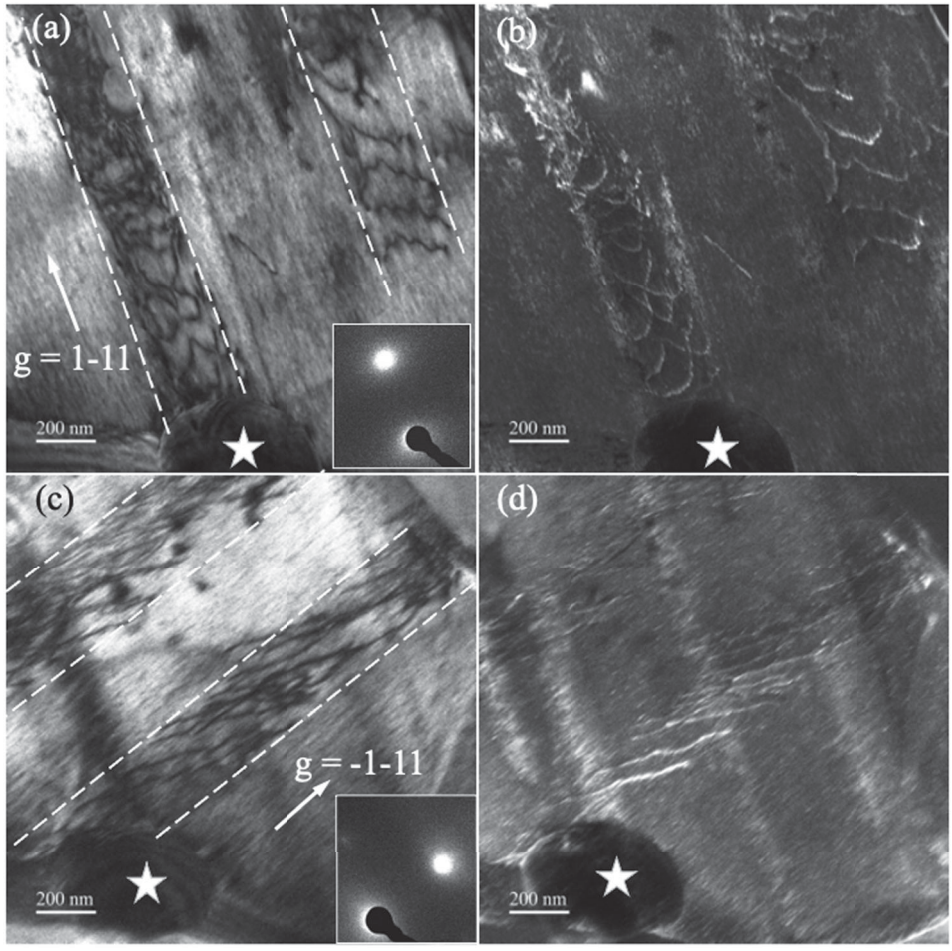

Figure 3. Dislocation analysis in room temperature nanoscratch-tested micron-grain HEO at ~150 mN applied normal load: (a, b) Two beam bright-field and weak-beam dark-field TEM images with g = 1–11 near [011] zone axis. (c, d) Two beam bright-field and weak-beam dark-field TEM images of the same region as in (a, b) with g = −1–11 near the [011] zone axis. The dislocations observed are $\frac{1}{2}<110>\{1\text{–}10\}$ type. The star marks the same location in the sample to guide the eye.

(visible as bright areas in the bright-field TEM image), and therefore appears darker and with more uniform image contrast, compared to the region outside the deformation zone. At an applied normal load of ~150 mN, micro-cracks are observed beneath the scratch groove (Figure 5(a)). A selected area diffraction pattern from this area shows diffraction rings corresponding to a rocksalt structure with no noticeable secondary phases (Figure 5(a), inset). The cracks display an intergranular propagation path, indicating grain boundaries play an important role in the deformation of nano-grain HEO (Figure 5(b)). EDS chemical analysis was performed near the micro-crack (Fig. S4), indicating cracking has no direct correlation with grain boundary segregation or secondary phase particles. Moderate dislocation activity is also observed in nano-grain HEO by bright- and dark-field STEM imaging (Figure 5(c,d), respectively). The dislocations were identified to be mostly screw type $\frac{1}{2}<110>\{1\text{–}10\}$ dislocations, same as those observed in micron-grain HEO.

Discussion

The dislocation density observed in micron-grained HEO is surprisingly high given that the mechanical test was non-ballistic and conducted at room temperature. High temperature deformation is commonly required to induce meaningful dislocation formation in ceramics, such as >1300°C to induce a dislocation density of 10^{12} m^{-2} in MgO [40] or >1300°C for 10^{12} m^{-2} in Al_2O_3 and 10 mol% Y_2O_3-ZrO_2 [41]. Room temperature dislocation densities comparable to those observed in this study are often only achievable in ceramics during high impact experiments, such as ball milling of MgO powders (10^{14} m^{-2}) [42] or ballistic impact testing in Al_2O_3 (10^{15} m^{-2}) [43]. To explain these significant

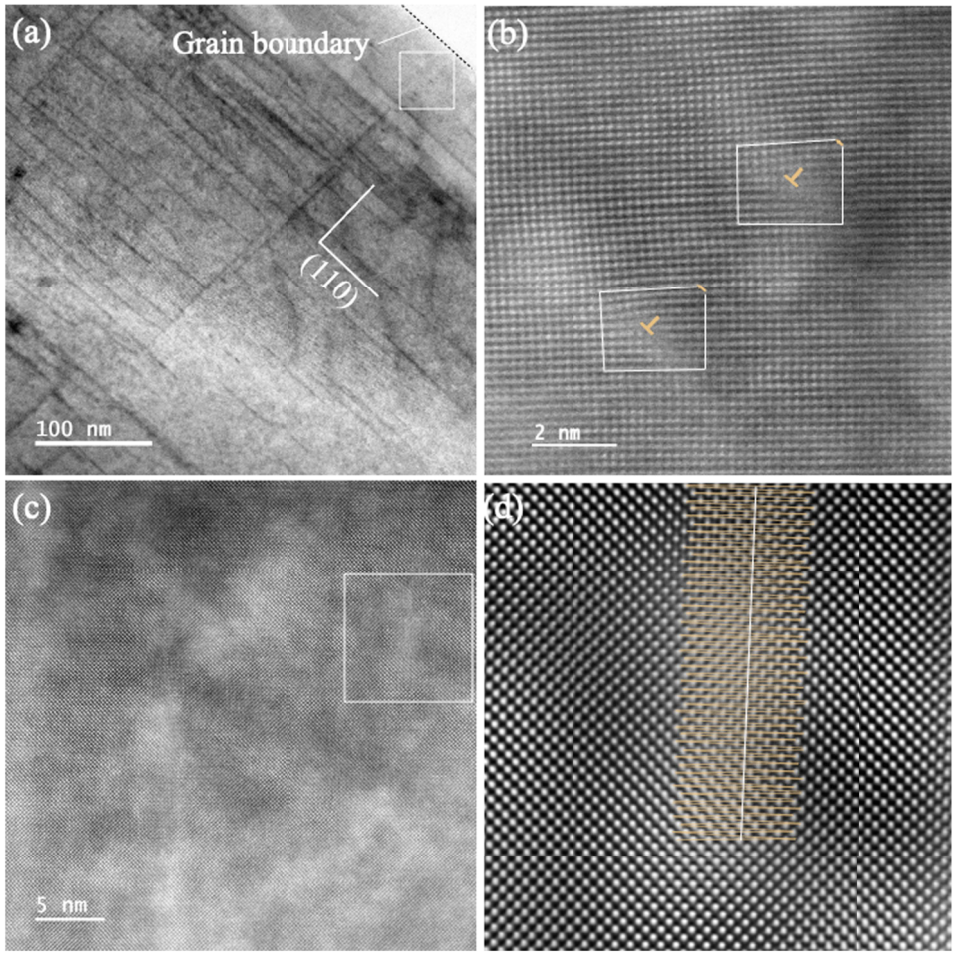

Figure 4. Dislocation structures in room temperature nanoscratch-tested micron-grain HEO at ∼ 150 mN applied normal load: (a) STEM image along [001] showing dislocations appear as straight lines parallel to the traces of {110} planes. (b) High-resolution STEM image of the white square region in (a), showing dislocation cores of edge $\frac{1}{2} < 110 > \{1\text{–}10\}$ dislocations. (c) High-resolution STEM image of screw dislocations. (d) IFFT image of the region marked by a white square in (c) showing the core of a screw dislocation marked by a white line.

differences in dislocation density and resulting deformation behavior, it is important to consider the differences between a simple single-cation oxide such as MgO and the complex multi-cation oxide (Co,Cu,Mg,Ni,Zn)O, even though they both exhibit rocksalt crystal structures. Specifically, we consider the lattice distortions known to exist in the (Co,Cu,Mg,Ni,Zn)O HEO, which are not present in pure MgO.

Lattice distortions are known to influence dislocation behavior and macroscopic deformation. For example, simulations by Qi and Chrzan show that Mo and Nb alloys with degenerate electron energy levels exhibit shear instability under applied stress due to the formation of lattice distortions [44]. Applied strain changes the energy band structure near the Fermi level. A critical strain exists in material with degenerate energy levels, above which a Jahn–Teller distortion forms, breaking the local symmetry and reducing the total electronic energy. This symmetry-breaking event leads to local shear instability and an increased likelihood of dislocation nucleation. Jahn–Teller distortions have been observed in (Co,Cu,Mg,Ni,Zn)O under ambient conditions [45,46], and have been attributed to degeneracy in the Cu^{2+} electronic configuration leading to compression and extension of the Cu-O bonds [47]. We propose that the tendency of (Co,Cu,Mg,Ni,Zn)O to form Jahn–Teller distortions will lead to shear instability and dislocation slip, facilitating mechanical deformation. Such lattice distortions are not expected to be present in MgO due to the lack of degenerate electronic configurations.

Grain size is an additional factor that can influence mechanical behavior. As grain size decreases, the volume fraction of material occupied by grain boundaries will increase. Grain boundaries are of higher energy than grain interiors, leading to mechanical behavior being highly sensitive to grain size [48]. Many ceramic materials exhibit significant changes in deformation

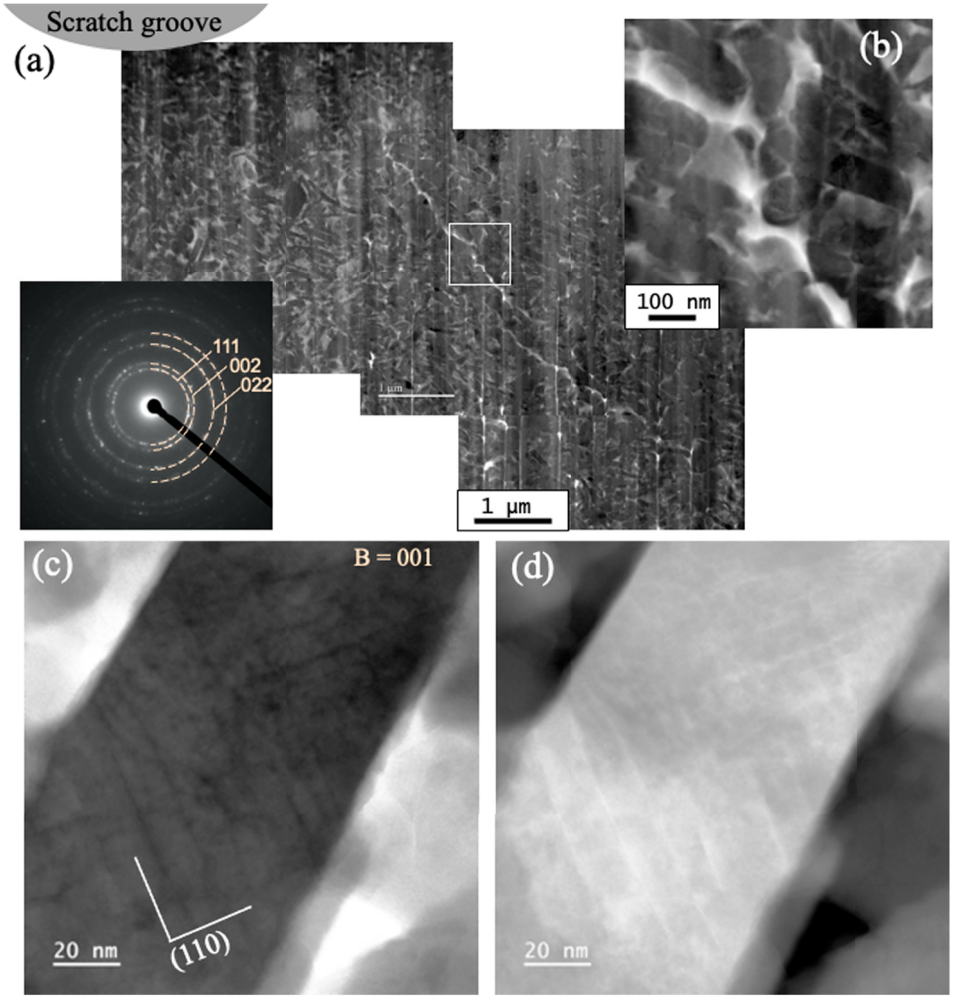

Figure 5. Cross-section of room temperature nanoscratch tested nano-grain HEO at ~150 mN applied normal load: (a) A montage of bright-field TEM images of the deformation zone below the scratch groove. Inset is the selected area diffraction pattern showing diffraction rings for single-phase rocksalt structure. (b) Zoomed in bright-field TEM of the region in (a) showing intergranular path of the micro-crack. (c, d) STEM bright and annular dark-field images of a nano-scale grain in the deformation zone. The dislocations within the grain are mostly screw type $\frac{1}{2} < 110 > \{1\text{–}10\}$ dislocations.

behavior below a critical grain size due to the emergence of deformation mechanisms that require less stress to activate than dislocation-mediated mechanisms [22,49]. This transition in deformation mechanism often results in an inverse Hall-Petch relationship. MgO, a constituent oxide in (Co,Cu,Mg,Ni,Zn)O with a similar rocksalt crystal structure, is known to exhibit a change in deformation mechanisms and an inverse Hall-Petch effect at small grain sizes [49]. Although the deformation mechanisms in nanocrystalline ceramics are not fully understood, crack propagation at grain boundaries and triple junctions as well as grain boundary sliding are commonly proposed [22,50]. In nano-grain HEO, we observe cracking in the deformation zone (Figure 5(a)), as well as indications of grain rearrangement by grain boundary sliding (Fig. S3), which are consistent with these earlier studies. In contrast, significant dislocation activity is observed in micron-grain HEO with no sign of cracking or grain boundary sliding behavior, indicating that dislocation-mediated deformation requires less stress to activate than the other two mechanisms when grain size is larger.

Conclusions

The local deformation mechanisms in micron-grain and nano-grain HEOs were investigated using room temperature nanoscratch deformation. Unlike most ceramics, (Co,Cu,Mg,Ni,Zn)O exhibits prominent and complex dislocation activity during this mechanical deformation. We attribute this unusual behavior to the multi-cation nature of HEOs and the Jahn–Teller lattice distortions

known to exist in these materials. The considerable dislocation activity observed in micron-grain HEO, which was identified to be predominantly $\frac{1}{2}<110>\{1–10\}$ screw type, indicates that (Co,Cu,Mg,Ni,Zn)O has the potential for significant dislocation-mediated deformation and strain hardening. Moreover, this unusual dislocation behavior in HEOs can provide a wide range of new opportunities for dislocation-mediated tuning of both functional and structural behavior not commonly feasible in conventional ceramics. Additionally, we find that deformation mechanisms change with grain size, with nano-grain samples exhibiting intergranular crack propagation in addition to some dislocation activity and grain boundary sliding. This change is attributed to an inverse Hall-Petch transition due to the increased grain boundary concentration. The observation of starkly different mechanical responses demonstrates that HEOs have the potential for diverse and highly tailorable mechanical behavior, providing a foundation for proper mechanical design of HEOs for engineering applications.

Supplementary information

Details of the experimental methods and additional S/TEM and EDS characterizations.

Acknowledgements

We acknowledge the use of facilities and instrumentation at the UC Irvine Materials Research Institute (IMRI) supported in part by the same NSF MRSEC (DMR-2011967) and technical assistance with the nanoscratch testing from Prof. Timothy Rupert and Dr Olivia Donaldson.

Disclosure statement

No potential conflict of interest was reported by the author(s).

Funding

The authors acknowledge financial support from the National Science Foundation (NSF-CMMI-2029966), the NSF Materials Research Science and Engineering Center (MRSEC) program through the UC Irvine Center for Complex and Active Materials (DMR-2011967), and a Graduate Assistance in Areas of National Need (GAANN) fellowship through the U.S. Department of Education (P200A-180043).

ORCID

Alexander D. Dupuy http://orcid.org/0000-0002-7405-5341

References

[1] Rost CM, Sachet E, Borman T, et al. Entropy-stabilized oxides. Nat Commun. 2015;6:8485.
[2] Dupuy AD, Wang X, Schoenung JM. Entropic phase transformation in nanocrystalline high entropy oxides. Mater Res Lett. 2019;7:60–67.
[3] Dupuy AD, Chellali MR, Hahn H, et al. Multiscale phase homogeneity in bulk nanocrystalline high entropy oxides. J Eur Ceram Soc. 2021;41:4850–4858.
[4] Sarkar A, Velasco L, Wang D, et al. High entropy oxides for reversible energy storage. Nat Commun. 2018;9:3400.
[5] Chen H, Fu J, Zhang P, et al. Entropy-stabilized metal oxide solid solutions as CO oxidation catalysts with high-temperature stability. J Mater Chem A. 2018;6:11129–11133.
[6] Braun JL, Rost CM, Lim M, et al. Charge-induced disorder controls the thermal conductivity of entropy-stabilized oxides. Adv Mater. 2018;30:1805004.
[7] Csanádi T, Castle E, Reece MJ, et al. Strength enhancement and slip behaviour of high-entropy carbide grains during micro-compression. Sci Rep. 2019;9:10200.
[8] Gild J, Braun J, Kaufmann K, et al. A high-entropy silicide: (Mo0.2Nb0.2Ta0.2Ti0.2W0.2)Si2. J Materiomics. 2019;5:337–343.
[9] Qin M, Yan Q, Wang H, et al. High-entropy monoborides: towards superhard materials. Scr Mater. 2020;189:101–105.
[10] Desissa TD, Meja M, Andoshe D, et al. Synthesis and characterizations of (Mg, Co, Ni, Cu, Zn)O high-entropy oxides. SN Appl Sci. 2021;3:733.
[11] Hong W, Chen F, Shen Q, et al. Microstructural evolution and mechanical properties of (Mg,Co,Ni,Cu,Zn)O high-entropy ceramics. J Am Ceram Soc. 2019;102:2228–2237.
[12] Pitike KC, Marquez-Rossy AE, Flores-Betancourt A, et al. On the elastic anisotropy of the entropy-stabilized oxide (Mg, Co, Ni, Cu, Zn)O compound. J Appl Phys. 2020;128:015101.
[13] Oshima Y, Nakamura A, Matsunaga K. Extraordinary plasticity of an inorganic semiconductor in darkness. Science. 2018;360:772–774.
[14] Sun B, Haunschild G, Polanco C, et al. Dislocation-induced thermal transport anisotropy in single-crystal group-III nitride films. Nat Mater. 2019;18:136–140.
[15] Sun L, Marrocchelli D, Yildiz B. Edge dislocation slows down oxide ion diffusion in doped CeO2 by segregation of charged defects. Nat Commun. 2015;6:6294.
[16] Armstrong MD, Lan K-W, Guo Y, et al. Dislocation-mediated conductivity in oxides: progress, challenges, and opportunities. ACS Nano. 2021;15:9211–9221.
[17] Porz L, Klomp A J, Fang X, et al. Dislocation-toughened ceramics. Mater Horiz. 2021;8:1528–1537.
[18] Appel F, Bethge H, Messerschmidt U. Dislocation motion and multiplication at the deformation of MgO single crystals in the high voltage electron microscope. Physica Status Solidi A. 1977;42:61–71.
[19] Foitzik A, Skrotzki W, Haasen P. Correlation between microstructure, dislocation dissociation and plastic anisotropy in ionic crystals. Mater Sci Eng A. 1989;113:399–407.
[20] Amodeo J, Merkel S, Tromas C, et al. Dislocations and plastic deformation in MgO crystals: a review. Crystals (Basel). 2018;8:240.
[21] Messerschmidt U. Dislocation dynamics during plastic deformation [Internet]. Berlin, Heidelberg: Springer Berlin Heidelberg; 2010 [cited 2022 Mar 21]. Available

from: http://link.springer.com/10.1007978-3-642-03177-9.
[22] Ryou H, Drazin JW, Wahl KJ, et al. Below the Hall–Petch limit in nanocrystalline ceramics. ACS Nano. 2018;12:3083–3094.
[23] Huang L, Bonifacio C, Song D, et al. Investigation into the microstructure evolution caused by nanoscratch-induced room temperature deformation in M-plane sapphire. Acta Mater. 2011;59:5181–5193.
[24] Huang L, Yao W, Mukherjee AK, et al. Improved mechanical behavior and plastic deformation capability of ultrafine grain alumina ceramics. J Am Ceram Soc. 2012;95:379–385.
[25] Beake BD, Harris AJ, Liskiewicz TW. Review of recent progress in nanoscratch testing. Tribol – Mater Surf Interfaces. 2013;7:87–96.
[26] Li C, Zhang Q, Zhang Y, et al. Nanoindentation and nanoscratch tests of YAG single crystals: an investigation into mechanical properties, surface formation characteristic, and theoretical model of edge-breaking size. Ceram Int. 2020;46:3382–3393.
[27] Ham RK. The determination of dislocation densities in thin films. Philos Mag. 1961;6:1183–1184.
[28] Meng Y, Ju X, Yang X. The measurement of the dislocation density using TEM. Mater Charact. 2021;175:111065.
[29] McGee TD. Grain boundaries in ceramic materials. In: Otte HM, Locke SR, editors. Materials science research. Boston, MA: Springer US; 1965. p. 3–32.
[30] Zhang R, Zhao S, Ding J, et al. Short-range order and its impact on the CrCoNi medium-entropy alloy. Nature. 2020;581:283–287.
[31] Savage MF, Neeraj T, Mills MJ. Observations of room-temperature creep recovery in titanium alloys. Metall Mater Trans A. 2002;33:891–898.
[32] Neeraj T, Mills MJ. Short-range order (SRO) and its effect on the primary creep behavior of a Ti–6wt.%Al alloy. Mater Sci Eng A. 2001;319–321:415–419.
[33] Messerschmidt U, Nishino Y, Imura T, et al. X-ray topographic in-situ observation of slip band propagation in MgO single crystals. Physica Status Solidi A. 1983;76:277–284.
[34] Höfling M, Trapp M, Porz L, et al. Large plastic deformability of bulk ferroelectric KNbO3 single crystals. J Eur Ceram Soc. 2021;41:4098–4107.
[35] Gerold V, Karnthaler HP. On the origin of planar slip in f.c.c. alloys. Acta Metall. 1989;37:2177–2183.
[36] Hong SI, Laird C. Mechanisms of slip mode modification in F.C.C. solid solutions. Acta Metall Mater. 1990;38:1581–1594.
[37] Lei Z, Liu X, Wu Y, et al. Enhanced strength and ductility in a high-entropy alloy via ordered oxygen complexes. Nature. 2018;563:546–550.
[38] Washburn J, Cass T. Dislocation dipoles in MgO. J Phys Colloques. 1966;27:C3-168–C3-177.
[39] Appel F, Bartsch M, Messerschmidt U, et al. Dislocation motion and plasticity in MgO single crystals. Physica Status Solidi A. 1984;83:179–194.
[40] Hüther W, Reppich B. Dislocation structure during creep of MgO single crystals. Philos Mag. 1973;28:363–371.
[41] Ikuhara Y. Oxide ceramics with high density dislocations and their properties. Mater Trans. 2009;50:1626–1632.
[42] Albanese-Kotar NF, Mikkola DE. Dissolution of comminuted magnesium oxide as affected by the density of dislocations introduced by various comminution methods. Mater Sci Eng. 1987;91:233–240.
[43] Crookes RG, März B, Wu H. Ductile deformation in alumina ceramics under quasi-static to dynamic contact impact. Mater Des. 2020;187:108360.
[44] Qi L, Chrzan DC. Tuning ideal tensile strengths and intrinsic ductility of bcc refractory alloys. Phys Rev Lett. 2014;112:115503.
[45] Rost CM, Rak Z, Brenner DW, et al. Local structure of the MgxNixCoxCuxZnxO(x = 0.2) entropy-stabilized oxide: An EXAFS study. J Am Ceram Soc. 2017;100:2732–2738.
[46] Berardan D, Meena AK, Franger S, et al. Controlled Jahn-Teller distortion in (MgCoNiCuZn)O-based high entropy oxides. J Alloys Compd. 2017;704:693–700.
[47] Rák Z, Maria J-P, Brenner DW. Evidence for Jahn-Teller compression in the (Mg, Co, Ni, Cu, Zn)O entropy-stabilized oxide: a DFT study. Mater Lett. 2018;217:300–303.
[48] Chaim R. Percolative composite model for prediction of the properties of nanocrystalline materials. J Mater Res. 1997;12:1828–1836.
[49] Ehre D, Chaim R. Abnormal Hall–Petch behavior in nanocrystalline MgO ceramic. J Mater Sci. 2008;43:6139–6143.
[50] Ratzker B, Wagner A, Sokol M, et al. Deformation in nanocrystalline ceramics: a microstructural study of MgAl2O4. Acta Mater. 2020;183:137–144.

Supplementary Information

High entropy oxide (Co,Cu,Mg,Ni,Zn)O exhibits grain size dependent room temperature deformation

Xin Wang[1], Justin Cortez[1], Alexander D. Dupuy[1], Julie M. Schoenung[1], William J. Bowman[1,2]*

[1] Department of Materials Science and Engineering, University of California, Irvine

[2] Irvine Materials Research Institute, University of California, Irvine, CA, United States

* E-mail: will.bowman@uci.edu

Methods

Materials preparation: HEO nanopowders were prepared through solid state methods, as described in our previous work [1]. These nanopowders were consolidated using a Fuji-825S spark plasma sintering (SPS) instrument. Nano-grain and micron-grain HEOs were heated to temperatures of 700 and 900 °C, respectively, at a heating rate of 200° C/min, under 100 MPa of pressure. Density of the consolidated samples was measured using Archimedes method. A SmartLab X-ray diffractometer (XRD) was used to examine the phase state of the samples.

Nanoscratch testing: A G200 Nanoindenter was used to perform room temperature scratch tests with a 25 μm diamond conical tip. The scan begins with an initial load of 0.5 mN. This load is increased at a constant rate of 0.67 mN/μm until the final load is 200 mN after the indenter has traveled 300 μm at a rate of 1 μm/s. A FEI Magellan 400 XHR scanning electron microscope (SEM) was used to characterize the morphology of scratch tracks.

Scanning transmission electron microscopy (S/TEM): S/TEM specimens were prepared with focused ion beam (FIB) with a FEI Quanta-3D dual-beam SEM, following routine trenching, lift out, thinning, and cleaning procedures. To examine the deformation microstructures at different load levels, cross-sectional S/TEM specimens were lifted out from two selected regions along the nanoscratch grooves, corresponding to normal loads of 50 and 150 mN for the nano-grain and the micron-grain HEO samples. S/TEM characterization was performed on the post-deformed HEOs using a JEOL JEM-2800, equipped with dual energy dispersive X-ray spectroscopy (EDS) detectors, or a JEOL JEM-ARM300F.

Supplementary Figures

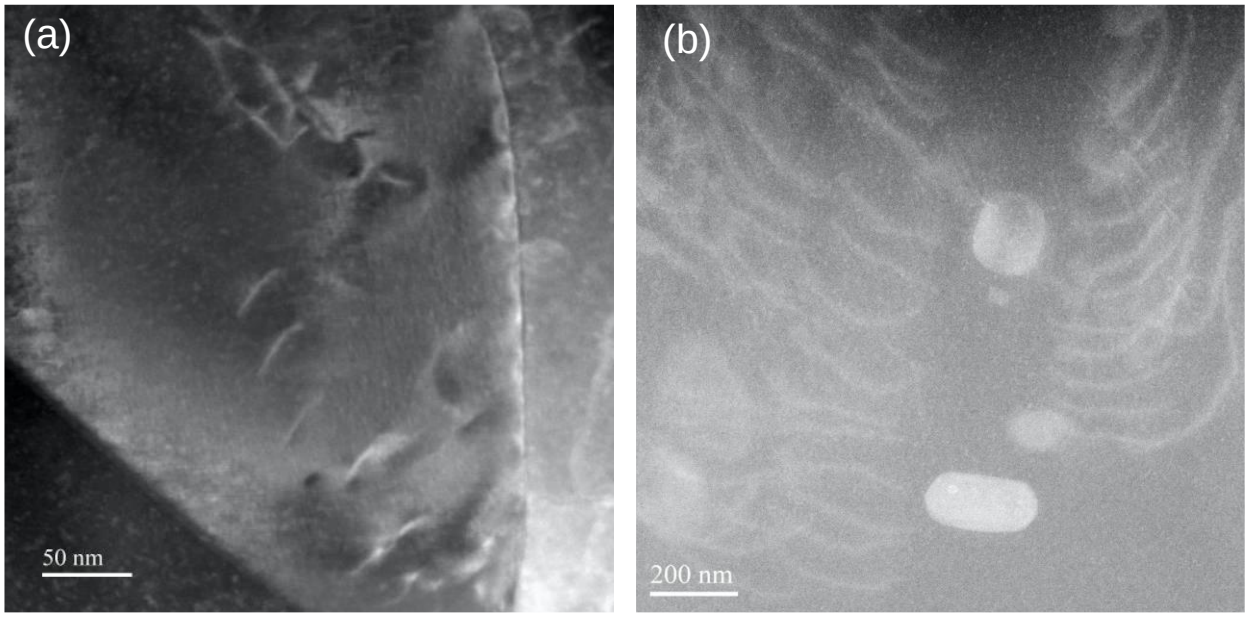

Fig. S1 (a and b) Dark field STEM images displaying the cross section of room temperature nanoscratch-tested micron-grain HEO (at ~50 mN applied normal load).

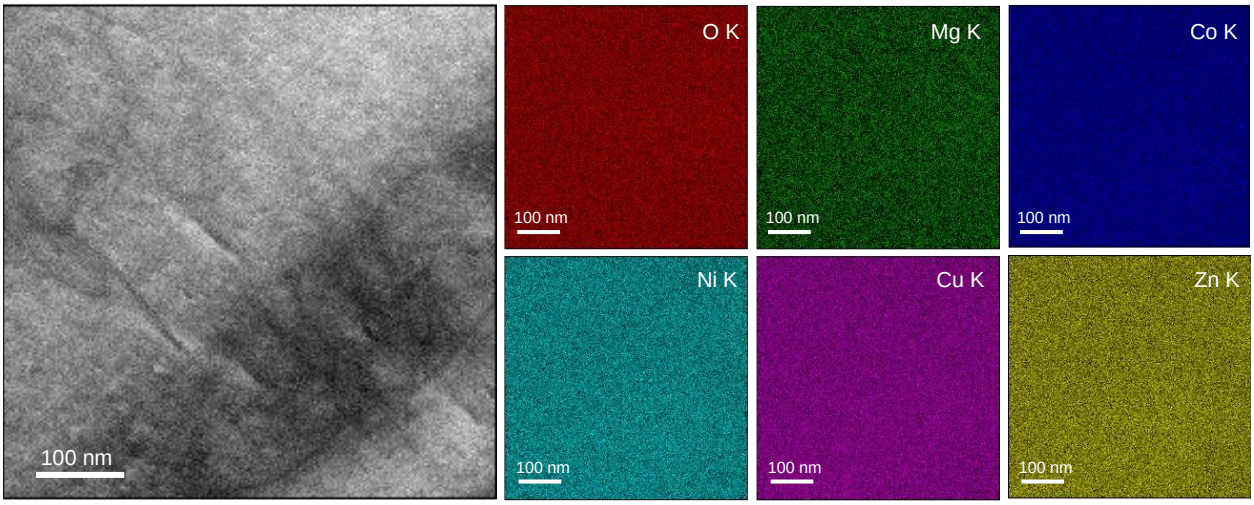

Fig. S2 STEM EDS analysis of room temperature nanoscratch-tested micron-grain HEO (at ~150 mN applied normal load) at the intersection of slip bands showing uniform distribution of all the elements.

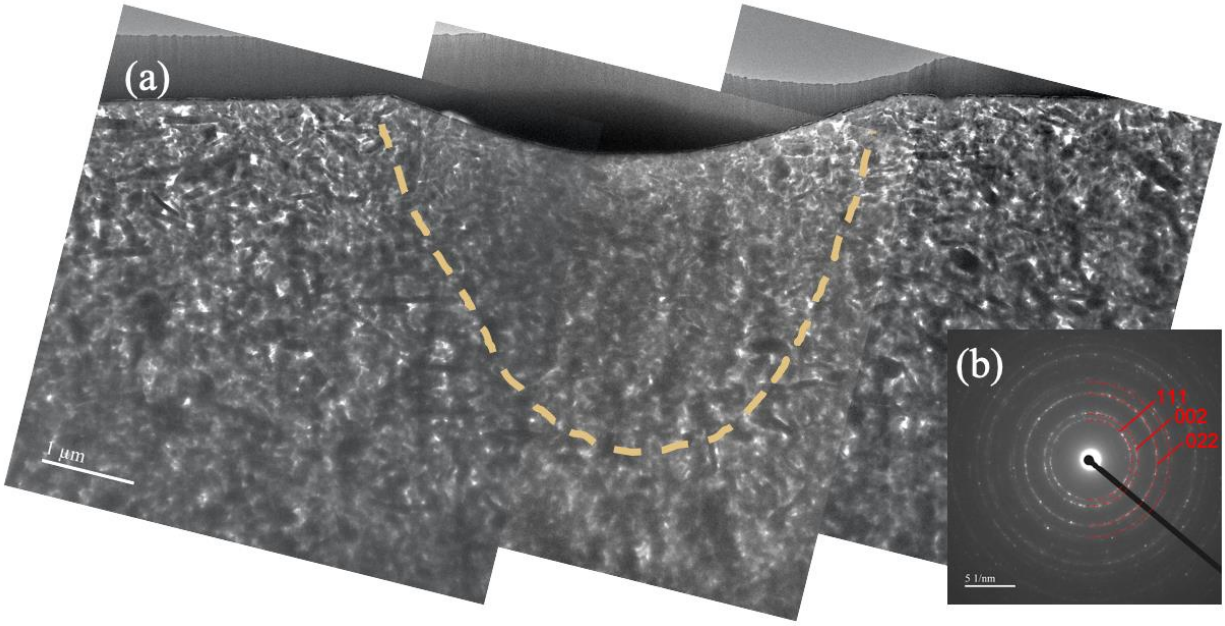

Fig. S3 (a) Cross-sectional bright field TEM images of nano-grain HEO (room temperature nanoscratch-tested at an applied normal load of ~50 mN). The deformation zone beneath the scratch groove is highlighted by a yellow dashed line. (b) The corresponding selected area diffraction pattern.

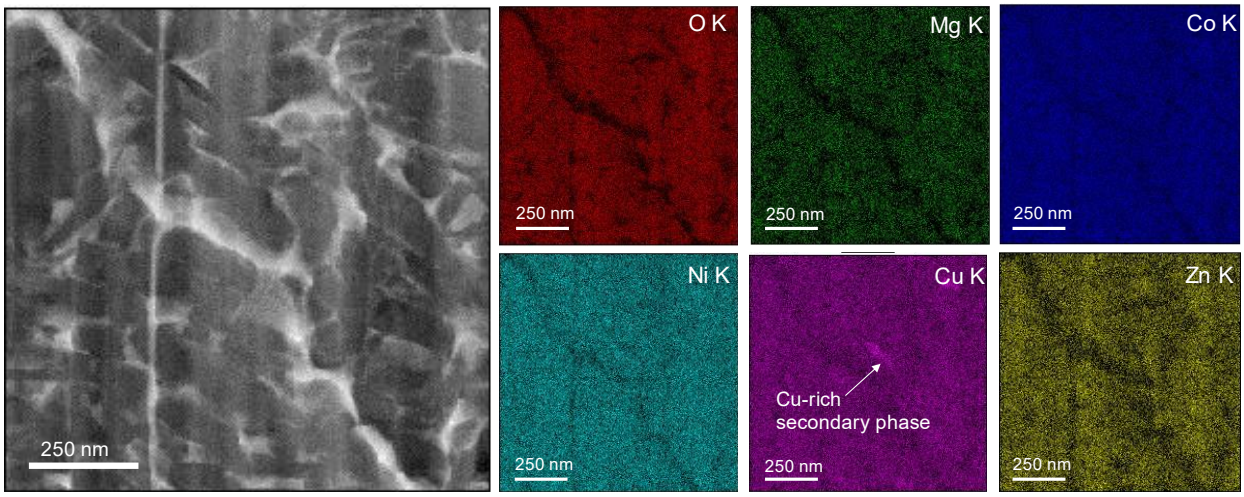

Fig. S4 STEM EDS analysis of room temperature nanoscratch-tested nano-grain HEO (at ~150 mN applied normal load) at a crack beneath the scratch groove.

Reference

[1] Dupuy AD, Wang X, Schoenung JM. Entropic phase transformation in nanocrystalline high entropy oxides. Mater Res Lett. 2019;7:60–67.